

Acetylcholinesterase Inhibitors: SAR and Kinetic Studies on ω -[*N*-Methyl-*N*-(3-alkylcarbamoyloxyphenyl)methyl]aminoalkoxyaryl Derivatives

Angela Rampa, Lorna Piazzini, Federica Belluti, Silvia Gobbi, Alessandra Bisi, Manuela Bartolini, Vincenza Andrisano, Vanni Cavrini, Andrea Cavalli, Maurizio Recanatini,* and Piero Valenti

Department of Pharmaceutical Sciences, University of Bologna, Via Belmeloro 6, 40126 Bologna, Italy

Received May 2, 2001

In this work, we further investigated a class of carbamic cholinesterase inhibitors introduced in a previous paper (Rampa et al. *J. Med. Chem.* **1998**, *41*, 3976). Some new ω -[*N*-methyl-*N*-(3-alkylcarbamoyloxyphenyl)methyl]aminoalkoxyaryl analogues were designed, synthesized, and evaluated for their inhibitory activity against both acetylcholinesterase (AChE) and butyrylcholinesterase (BuChE). The structure of the lead compound (xanthostigmine) was systematically varied with the aim to optimize the different parts of the molecule. Moreover, such a structure–activity relationships (SAR) study was integrated with a kinetic analysis of the mechanism of AChE inhibition for two representative compounds. The structural modifications lead to a compound (**12b**) showing an IC_{50} value for the AChE inhibition of 0.32 ± 0.09 nM and to a group of BuChE inhibitors also active at the nanomolar level, the most potent of which (**15d**) was characterized by an IC_{50} value of 3.3 ± 0.4 nM. The kinetic analysis allowed for clarification of the role played by different molecular moieties with regard to the rate of AChE carbamylation and the duration of inhibition. On the basis of the results presented here, it was concluded that the cholinesterase inhibitors of this class possess promising characteristics in view of a potential development as drugs for the treatment of Alzheimer's disease.

Introduction

The study of new agents useful to treat Alzheimer's disease (AD) is one of the most active research fields in both pharmaceutical industry and academia. AD is a progressive neurodegenerative syndrome associated with aging leading to the most common form of senile dementia. The disease is characterized by the presence of some neuropathological markers detected in the brain of AD patients, which are the β -amyloid (β A) plaques and the neurofibrillary tangles. A pathogenic role is ascribed to these lesions, and many research programs focused on drugs able to modify the course of the disease are targeting both their formation and neurotoxicity.¹

On the other hand, a number of pharmacological agents are already available to treat AD, and although they are not able to block the progression of the neurodegeneration, still they are of help in managing the symptoms of the disease. All these drugs (Chart 1) can be considered as outcomes of the so-called *cholinergic hypothesis*,² that, at least in its earliest formulation,³ predicted a favorable effect for compounds able to sustain the central cholinergic tone. Tacrine, donepezil, and rivastigmine are acetylcholinesterase (AChE) inhibitors that increase the levels of acetylcholine (ACh) at the synapse by blocking the breakdown of the neurotransmitter. Tacrine and donepezil act through a competitive mechanism, while rivastigmine is an acylating inhibitor able to covalently modify the enzyme by transferring its carbamoyl group to the serine hydroxyl present in the active site.⁴

* To whom correspondence should be addressed. Tel: +39 051 2099720. Fax: +39 051 2099734. E-mail: mreca@alma.unibo.it.

Chart 1. Drugs Presently Marketed for the Treatment of AD

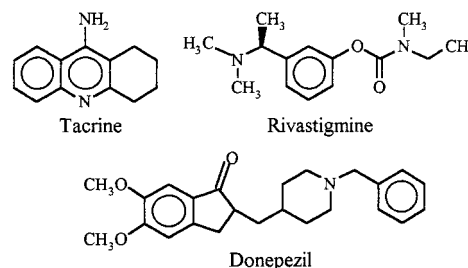
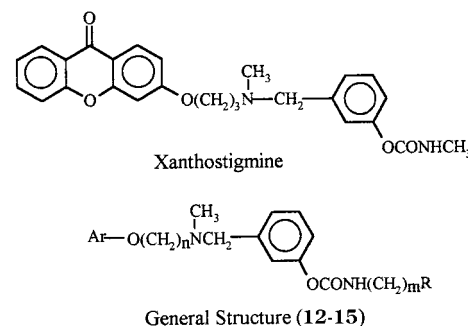
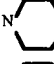

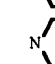
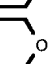


Chart 2. Structures of ω -[*N*-Methyl-*N*-(3-alkylcarbamoyloxyphenyl)methyl]aminoalkoxyaryl Derivatives



In previous papers,⁵ we introduced and studied a class of *N*-methyl-*N*-(3-carbamoyloxyphenyl)methylamino derivatives characterized by the presence of a heteroaryl moiety linked to the tertiary amino nitrogen through an alkoxy chain (Chart 2). The structure–activity relationships (SAR) of this series of AChE inhibitors

Table 1. Physicochemical and Analytical Data of the Compounds Studied

compd	Ar ^a	<i>n</i>	<i>m</i>	R	mp (°C)	yield (%)	formula	analysis
12a	Z	6	0	CH ₃	104–106	50	C ₂₉ H ₃₂ N ₂ O ₅ ^b	C, H, N
12b	Z	7	0	CH ₃	118–120	50	C ₃₀ H ₃₅ ClN ₂ O ₅ ^c	C, H, N
12c	Z	8	0	CH ₃	152–154	50	C ₃₁ H ₃₇ ClN ₂ O ₅ ^c	C, H, N
12d	Z	9	0	CH ₃	129–131	50	C ₃₂ H ₃₉ ClN ₂ O ₅ ^c	C, H, N
12e	Z	10	0	CH ₃	138–140	50	C ₃₃ H ₄₁ ClN ₂ O ₅ ^c	C, H, N
12f	Z ₁	3	0	CH ₃	155–158	20	C ₂₆ H ₂₉ ClN ₂ O ₄ ^c	C, H, N
12g	Z ₂	3	0	CH ₃	135–137	30	C ₂₆ H ₃₁ ClN ₂ O ₃ ^c	C, H, N
12h	Z ₃	3	0	CH ₃	136–139	30	C ₂₃ H ₂₇ ClN ₂ O ₃ ^c	C, H, N
12i	Z ₄	3	0	CH ₃	121–124	20	C ₁₉ H ₂₅ ClN ₂ O ₃ ^c	C, H, N
12j	Z ₅	3	0	CH ₃	100–101	20	C ₂₅ H ₂₈ N ₂ O ₃ ^b	C, H, N
13	Z	-	0	CH ₃	90–93	30	C ₂₇ H ₂₅ ClN ₂ O ₅ ^c	C, H, N
14	Z	-	0	CH ₃	158–160	40	C ₂₇ H ₂₇ ClN ₂ O ₅ ^c	C, H, N
15a	Z	3	6		94–97	15	C ₃₅ H ₄₃ N ₃ O ₆ ^b	C, H, N
15b	Z	3	7		66–68	20	C ₃₆ H ₄₅ N ₃ O ₆ ^b	C, H, N
15c	Z	3	8		32–33	15	C ₃₇ H ₄₇ N ₃ O ₆ ^b	C, H, N
15d	Z	3	9		35–36	20	C ₃₈ H ₄₉ N ₃ O ₆ ^b	C, H, N

^a See Chart 2 (General Structure) for the definitions of Ar, *n*, *m*, and R. ^b Free base (crystallizing from ligroin). ^c Hydrochlorides (crystallizing from methanol–ether).

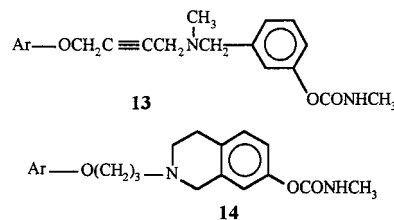
were analyzed, and some conclusions were drawn regarding the features of different parts of the molecular skeleton.^{5b} In particular, the dibenzopyran-4-one ring, a three-carbon-atom chain, and a methyl group on both the amino and the carbamic nitrogen atoms provided the best results in term of inhibitory activity against isolated AChE (IC₅₀ = 0.30 nM for the most potent compound,^{5b} xanthostigmine in Chart 2). The relevant level of AChE inhibitory potency reached by some compounds of the series prompted us to further explore the SAR of the class, also paying attention to some aspect of AChE inhibition that recently emerged in connection with the use of anticholinesterase agents in the treatment of AD. We thus decided to introduce modifications in the linker chain, the carbamoyl substituent, and the aryl moiety of xanthostigmine and to study the effects of such changes on the AChE inhibitory activity. The ability to inhibit butyrylcholinesterase (BuChE) was tested as well, to assess the selectivity of the compounds. Finally, a kinetic study was carried out on two representative members of the series, aimed at characterizing the mechanisms of the AChE inhibitory action for the xanthone-derived class of anticholinesterases.

Inhibitor Design. In the title compounds, the alkoxy chain linking the aryl moiety to the tertiary amino group was lengthened to allow the aryl ring to contact the Trp279 side chain at the entrance of the AChE gorge. This aromatic residue together with other ones (Tyr70, Tyr121) is considered to constitute an essential part of the AChE peripheral binding site,⁶ and recent studies have shown that inhibitors binding to this site are able to block the βA aggregation induced by AChE.⁷ A three-dimensional model of the binary complex between AChE and xanthostigmine^{5b} showed that by

properly extending the alkoxy chain of aminoalkoxyaryl derivatives, it is possible to reach the external site, in such a way as the heteroaryl moiety has the possibility to establish π-stacking interactions with the indole ring of Trp279. Accordingly, we designed the subset of compounds **12a–e** characterized by *n* = 6–10 (Table 1).

In our previous work on the same class of carbamic AChE inhibitors,^{5b} we studied the SAR of the heteroaryl moiety by replacing the xanthone ring with several different nuclei based on the benzopyran skeleton. In the series presented here, we aimed at probing the relevance of the benzopyran oxygenated functions by introducing a benzophenone (compound **12f**) or other aromatic moieties (compounds **12g–j**) as aryl groups.

To explore whether the AChE gorge could tolerate less flexible analogues, an ethyne fragment was introduced within the linker chain (compound **13**). Moreover, the tertiary amine function was included in a tetrahydroisoquinoline nucleus, in such a way as to mimic the *N*-methyl-*N*-benzyl fragment of xanthostigmine through a partially saturated ring (compound **14**).



Substituents on the carbamic nitrogen of covalent AChE inhibitors are known to affect the regeneration time of the enzyme, in the sense that the presence of

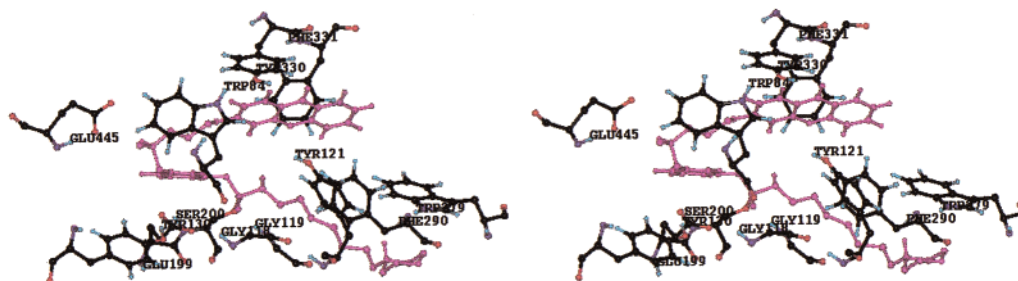


Figure 1. Stereoview of the binary complex between **15b** (magenta) and AChE. The carbamic *N*-heptyl chain can position the protonated morpholine ring at a suitable distance from the indole ring of Trp279 to give a π -cation interaction. The model was obtained by following the procedure described in ref 5b for inhibitor docking and complex minimization.

longer carbamic *N*-alkyl chains increases the recovery time.⁸ Actually, in the series of heteroarylcarbamic derivatives previously published,^{5b} we detected such an effect. Moreover, recently, Bartolucci et al.⁹ reported the crystal structure of a carbamoylated AChE bearing a dimethylmorpholinooctylcarbamic moiety covalently bound to the catalytic serine of the enzyme. From this study, it clearly appeared that the protonated morpholine interacted with the indole side chain of Trp279 via a π -cation interaction. Thus, we attempted to combine an increased duration of action with the possibility to contact the AChE peripheral site by designing compounds **15a–d**, in which the carbamic *N*-alkyl chain varies from 6 to 9 carbon units. Additionally, the terminal morpholino group might counterbalance the increase of lipophilicity due to the rather long alkyl chains and improve the pharmacokinetic properties of the compounds.¹⁰

To theoretically verify the binding hypothesis of the above long chain morpholinoalkyl carbamates, we modeled the tetrahedral intermediate formed by compound **15b** in the AChE gorge. From the docking model shown in Figure 1, it clearly appears that the morpholino ring has the possibility to contact the peripheral site, provided that the *N*-alkyl chain is of appropriate length.

Chemistry. The synthesis of the studied compounds was accomplished as illustrated in Scheme 1.

The selected hydroxy-derivatives were treated with 1-bromo-*o*-chloroalkanes or *o*-dibromoalkanes (according to commercial availability) in the presence of K_2CO_3 to afford *o*-haloalkoxy-derivatives **1a–j**, which were treated with NaI in refluxing methyl ethyl ketone to give the corresponding *o*-iodoalkoxy-intermediates **2a, 2f–j, 7**. These compounds were then condensed with *N*-(3-hydroxybenzyl)methylamine^{5b} to afford **3a–j, 8** or with 7-nitro-1,2,3,4-tetrahydroisoquinoline¹¹ to give **9**. The nitro-derivative **9** was hydrogenated with Pd/C to **10**, which was then diazotated to afford **11**. The hydroxy-derivatives **3a–j, 11** were treated with methyl isocyanate to give the desired compounds **12a–j, 14**.

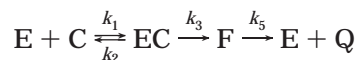
3-Hydroxyxanthone was treated with $BrCH_2C\equiv CH$ in the presence of K_2CO_3 to afford **4**, which was condensed with *N*-(3-benzyloxybenzyl)methylamine to afford **5**, debenzylated to **6**, and then treated with methyl isocyanate to give **13**.

Compound **8** was treated with the appropriate *o*-morpholinoalkylisocyanates¹⁰ to afford compounds **15a–d**.

Enzyme Inhibition. The inhibitory activity against AChE of the newly synthesized compounds was studied using the method of Ellmann et al.¹² to determine the rate of hydrolysis of acetylthiocholine (ATCh) in the

presence of the inhibitor. The selectivity of the compounds was also tested by determining their inhibitory activity against BuChE.

The mechanism of the AChE inhibition was studied in depth for two representative compounds of the series (**12a** and **15b**). As previously reported,¹³ the inhibition of AChE by carbamates involves a reversible complex (EC) formation, followed by carbamoylation of the enzyme and production of a covalent adduct (F). The carbamoylated enzyme is then hydrolyzed to regenerate the free enzyme. The whole mechanism can be represented as follows:



After the reversible complex formation (EC; equilibrium constant: $K_C \equiv k_2/k_1$), the carbamoylation phase of the reaction is considerably more rapid than the decarbamoylation phase (i.e., $k_3 > k_5$), and the two phases can be characterized separately.^{13b,c} Therefore, we investigated on both the first kinetic phase (carbamoylation) of the inhibition process, by determining k_3 , and the decarbamoylation stage, by determining k_5 , with the final aim to compare the mode of action of the new inhibitors with that of the reference compound physostigmine.

To characterize the carbamoylation step, a traditional stopped time assay^{13b} was performed, in which AChE and inhibitor were mixed in the assay buffer, and aliquots were transferred to the spectrophotometer cell at various times for the determination of the residual AChE activity. The data were fitted to the following equation

$$R = R_0 \exp(-k_{\text{obs}}t) + R_{\infty} \quad (1)$$

where R , R_0 , and R_{∞} are ratios of the inhibited enzyme activity (v_i) to the control activity (v_0) at times t , 0, and ∞ , respectively. In this way, the values of the observed pseudo-first-order inhibition rate constant (k_{obs}) for each concentration of inhibitor were obtained. Double reciprocal plots of k_{obs} versus inhibitor concentration ($[I]$) were then used to compute k_3 and K_C from the intercept and from the ratio of the slope to the intercept, respectively, according to the equation:

$$1/k_{\text{obs}} = K_C/k_3 \cdot 1/[I] + 1/k_3 \quad (2)$$

Concerning the characterization of the last stage of inhibition (decarbamoylation), the carbamoylated enzyme prepared by incubating AChE with the inhibitor

Table 2. Inhibitory Activity on Isolated AChE and BuChE and IC₅₀ Ratio of the Compounds Studied

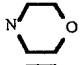
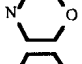
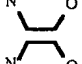

compd	Ar	n	m	R	IC ₅₀ (nM) AChE	IC ₅₀ (nM) BuChE	IC ₅₀ ratio BuChE/AChE
12a	Z	6	0	CH ₃	1.4 ± 0.3	13.9 ± 1.1	9.9
12b	Z	7	0	CH ₃	0.32 ± 0.09	16.5 ± 1.4	51.6
12c	Z	8	0	CH ₃	6.8 ± 0.7	25.2 ± 3.0	3.7
12d	Z	9	0	CH ₃	11.7 ± 0.5	48.3 ± 3.4	4.1
12e	Z	10	0	CH ₃	21.8 ± 2.1	31.6 ± 1.7	1.4
12f	Z ₁	3	0	CH ₃	5.4 ± 0.8	24.5 ± 2.6	4.5
12g	Z ₂	3	0	CH ₃	24.7 ± 2.9	22.1 ± 0.9	0.9
12h	Z ₃	3	0	CH ₃	82.6 ± 4.1	205 ± 27	2.5
12i	Z ₄	3	0	CH ₃	79.6 ± 3.7	24.8 ± 2.2	0.3
12j	Z ₅	3	0	CH ₃	54.6 ± 1.8	42.6 ± 3.0	0.8
13	Z	-	0	CH ₃	210 ± 15	529 ± 91	2.5
14	Z	-	0	CH ₃	12.4 ± 1.3	34.1 ± 3.0	2.7
15a	Z	3	6		21.1 ± 2.6	7.5 ± 0.8	0.35
15b	Z	3	7		26.2 ± 2.2	4.9 ± 0.3	0.2
15c	Z	3	8		27.4 ± 2.9	3.9 ± 0.4	0.1
15d	Z	3	9		29.3 ± 4.8	3.3 ± 0.4	0.1
phys.					14.1 ± 0.2	23.1 ± 1.0	1.6

Table 3. Kinetic and Thermodynamic Constants for the AChE Inhibition

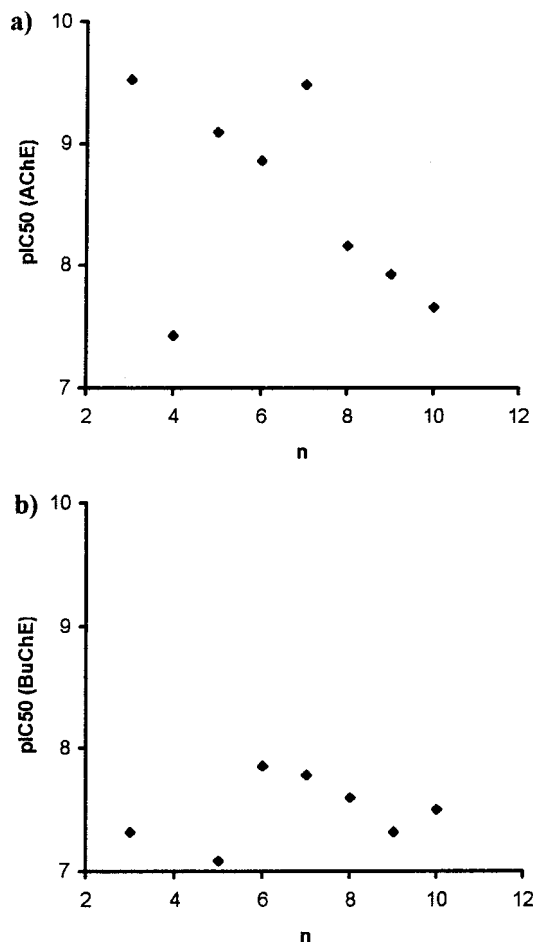
compd	K _C (nM)	k ₃ (min ⁻¹)	k ₅ (h ⁻¹)
12a	6.4 ± 0.5	2.3 ± 0.3	0.77 ± 0.05 0.06 ± 0.01
15b	27.2 ± 3.2	0.11 ± 0.01	
physostigmine	33.5 ± 2.7	0.41 ± 0.05	0.43 ± 0.02

intermediate level of potency between **12f** and **12h–j**. The selectivity with respect to the BuChE inhibition is almost negligible in this subset.

Compounds **13** and **14** containing some constraints that hinder the mutual flexibility of the extreme aryl and phenylcarbamic groups show different potencies on both the cholinesterases but the same (almost null) selectivity. The introduction of a rigid linear ethyne moiety in the linking chain is detrimental for both the AChE and BuChE inhibitory activities, indicating that a flexible chain is necessary. On the other hand, incorporation of the tertiary amino group into a saturated ring is not likewise deleterious, even if the activity decreases with respect to the lead compound, and is also lower than that of other analogues (the subset **12a–d**).

Finally, the variation of the length of the carbamic *N*-substituent has a remarkable effect on the selectivity of the inhibitors, as compounds **15a–d** show a higher inhibitory activity on BuChE than on AChE. Another interesting aspect of the IC₅₀ data of this subset is that the number of methylene units (*m* = 6–9) of the ω -morpholinoalkyl-substituent influences only slightly the inhibitory potency, which ranges from 21.1 to 29.3 nM against AChE, and from 3.3 to 7.5 nM against BuChE. Compound **15d** is the most potent BuChE inhibitor of this class of carbamic derivatives, showing an IC₅₀ value of 3.3 nM.

Mechanism of AChE Inhibition. The equilibrium and rate constants (*K_C* and *k₃*, respectively) of physostigmine, **12a**, and **15b** were determined from eq 2 following the method reported by Feaster and Quinn^{13b} (Table 3). From the plots of Figure 3, it appears that the two heteroaryloxyalkylamino compounds show a time-dependent pattern of inhibition, which is similar

**Figure 2.** Plots of pIC₅₀ values for AChE (a) and BuChE (b) inhibition against the number of methylene units of compounds **12a–e**. IC₅₀ values for the analogues with 3–5 methylene units were taken from ref 5b.

to that of physostigmine. The time course of the inhibition is characterized by an increase until to a steady state, which is reached after 20 min, almost 2 h, and 40 min, in the case of **12a**, **15b**, and physostigmine, respectively. The stability constants of the inhibitor–

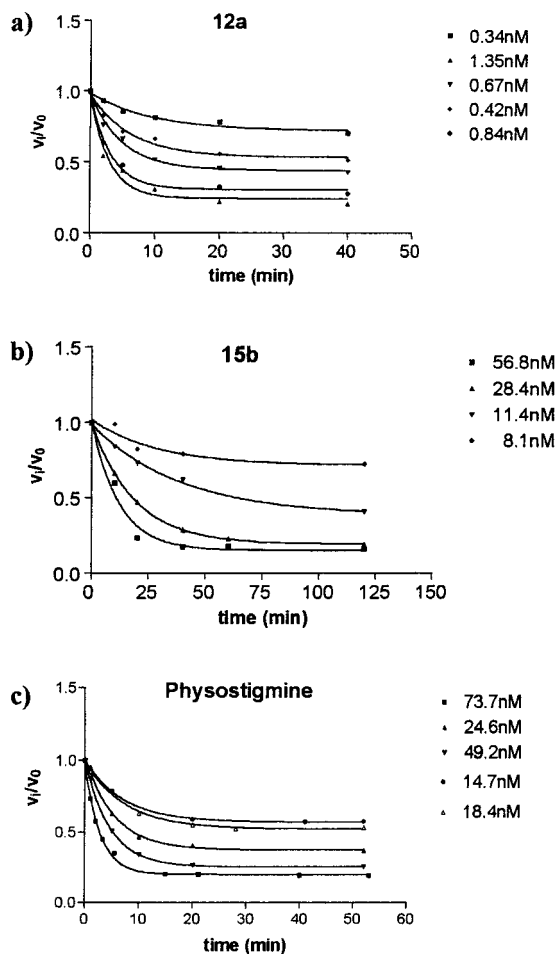


Figure 3. Time course of AChE inhibition by **12a** (a), **15b** (b), and physostigmine (c).

AChE complex (K_C) and the rate constant of the carbamoyl-enzyme formation (k_3) were different for **12a**, **15b**, and physostigmine, compound **12a** showing the highest rate of carbamoyl-AChE formation, nearly 20 times higher than **15b**. To further explore some aspects of the carbamoylation of cholinesterases, the rate of formation of the carbamoyl adduct (k_{obs}) with BuChE for the 7-morpholinoheptyl-derivative **15b** (at 13 nM inhibitor concentration) was also measured. The k_{obs} resulted equal to 1.009 min^{-1} for BuChE carbamoylation, while the same kinetic parameter for AChE was 0.0243 min^{-1} .

To study the last step of the enzymatic reaction, the carbamoyl-AChE adducts formed by **12a** and by **15b** were hydrolyzed to regenerate the free enzyme. The percentage of recovered cholinesterase activity was plotted against time (Figure 4). According to previous studies,^{14,5b} the velocity of this step was related to the length of the carbamate *N*-alkyl chain. Compound **12a** (bearing the *N*-methylcarbamoyl substituent) showed a two-phase activity recovery, with $t_{1/2}$ values of 0.9 and 11.2 h, respectively, which seems to account for a two-site binding mechanism. Instead, the 7-morpholinoheptyl-derivative **15b** was still inhibited after 96 h (Figure 4). This last behavior was in agreement with the data reported for long chain analogues of physostigmine.⁸

Discussion

One of the aims of the present work was to extend the study of the SAR of the ω -[*N*-methyl-*N*-(3-alkylcar-

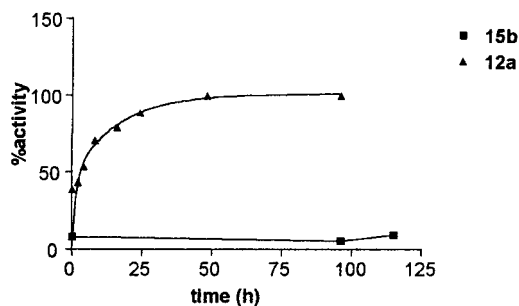


Figure 4. Time course of AChE regeneration after inhibition by **12a** and **15b**.

bamoyloxyphenyl)methyl]aminoalkoxyaryl AChE inhibitors by appropriately varying some selected structural features of the molecules. The results presented in Table 2, integrated with those reported in the previous article on the same class of compounds,^{5b} allow us to definitely assess the relative importance of the different parts of the molecules.

The length of the chain linking the (hetero)aryloxy moiety to the basic nitrogen influences substantially the AChE inhibitory potency, even if a simple correlation between number of carbon units and activity does not exist (Figure 2a). The compounds characterized by four and seven methylene units, and showing IC_{50} values equal to 37 nM ^{5b} and 0.32 nM (**12b**), respectively, fall clearly out of the otherwise linear plot of Figure 2a, indicating that some specific (unfavorable or favorable) interaction strongly affects their binding to the AChE gorge. These data suggest that the length and the flexibility of the spacer chain affect in some rather unpredictable way the interactions of the compounds with the residues lining the gorge and do not allow the establishment of a correlation with physicochemical properties (like lipophilicity), due also to the simultaneous variation of size and lipophilicity in the subset. The essential role of the intermediate chain flexibility is pointed out by the weak anti-AChE activity of compound **13** carrying the ethyne fragment ($IC_{50} = 210 \text{ nM}$). It is interesting to note that **13** has almost the same value of calculated¹⁵ $\log P$ (4.93) as xanthostigmine (4.48). The inclusion of the tertiary amine nitrogen in a cycle, like in compound **14**, affects the binding capability less than the stiffening of the chain, indicating that the tetrahydroisoquinoline ring mimics a conformation of the *N*-methyl-*N*-benzylamine fragment compatible with a correct orientation of the molecule in the enzyme active site.

With regards to the aryl moiety, it appears from both the data of Table 2 and the consideration of the previous results^{5b} that the presence of polar groups in this part of the molecules is essential for a strong binding to AChE. In fact, all the compounds lacking any polar (generally oxygen) atom in the aryl ring lose activity for at least 1 order of magnitude. In an attempt to explain in terms of molecular properties the effects of the variation of the aryl moieties on the AChE inhibitory activity, we calculated the frontier orbitals for model compounds representing the derivatives having the same values of n (3), m (0), and R (CH_3), and variable aromatic nucleus. The HOMO and LUMO energies for the different aryloxymethyl fragments (including those of the corresponding compounds studied in ref 5b) are

Table 4. Frontier Orbital Energies of the Different Aryl Moieties

model compd	compd	$E(\text{HOMO})^a$ (kcal/mol)	$E(\text{LUMO})^a$ (kcal/mol)
	(ref 5b)	-9.2237	-0.6828
	(ref 5b)	-9.4540	-0.9246
	(ref 5b)	-9.2011	-0.9110
	(ref 5b)	-9.4383	-0.5254
	(ref 5b)	-9.3537	-0.6864
	12f	-9.3568	-0.3810
	12g	-9.0769	-0.0804
	12h	-8.5933	-0.4155
	12i	-9.1140	0.3578
	12j	-8.8296	-0.0582

^a Energy values calculated by means of the PM3 program.²⁰

reported in Table 4. There is no quantitative correlation between pIC_{50} and HOMO or LUMO energies, but a trend clearly emerges: it appears that the most potent AChE inhibitors have the most negative values of both orbital energies, while the least active derivatives show the least negative values of both $E(\text{HOMO})$ and $E(\text{LUMO})$. This behavior might be interpreted in the sense that compounds interact better with the active site gorge, if they are able to favorably accept electrons in their LUMO. Thus, the involvement of the LUMO (which, in the whole molecules, is localized on the aryl moiety) in the variation of activity might confirm the hypothesis advanced in the previous paper^{5b} that this part of the molecule can establish π -stacking interactions with aromatic residues lining the AChE gorge. On the other hand, no relationships with lipophilicity or size can be found.

Compounds **12a–j**, **13**, and **14** considered thus far do not seem to discriminate between AChE and BuChE, as their BuChE/AChE IC_{50} ratios range between 10 and 0.3, with the only exception of **12b** (51.6). Within these small figures, three compounds (**12g**, **12i**, **12j**) show a preference for the BuChE active site. Instead, all the compounds characterized by long variable ω -morpholinoalkyl chains on the carbamic nitrogen (**15a–d**) are slightly selective for BuChE, displaying also the ten-

dency to increase selectivity with the chain length. However, these compounds are quite effective BuChE inhibitors active at the nanomolar level ($\text{IC}_{50} = 3.3\text{--}7.5$ nM). Eptastigmine, the *N*-heptyl analogue of physostigmine, has an IC_{50} against BuChE of 5 nM,¹⁶ and, recently, Yu et al. reported a phenserine-based selective BuChE inhibitor showing an IC_{50} value of 1 nM.¹⁷ Compound **15d** ($\text{IC}_{50} = 3.3$ nM) can thus be considered one of the most potent BuChE inhibitors currently known, and it is worth further study aimed at improving its selectivity, at the light of the recent hypothesis regarding a role for BuChE inhibitors in the treatment of AD.^{17,18} In particular, Giacobini proposed that severe cases of AD might be treated by blocking the glial BuChE with selective inhibitors, as such agents would produce an increase of the brain levels of ACh without eliciting cholinergic side effects.¹⁸

The results of the kinetic experiments performed with physostigmine, **12a**, and **15b** can be used to tentatively explain some aspects of the AChE inhibition mechanisms by the different carbamates, which might then help to understand the different inhibitory potencies. Indeed, the structure of the three molecules plays a role in differentiating their inhibitory potency (IC_{50} values) and also their kinetic mechanism of action. Physostigmine and **15b** are widely different in structure and size; still their IC_{50} values differ by less than two times. On the contrary, **12a**, not much different from **15b**, shows a 10-fold potency with respect to physostigmine. However, the inhibitor forming the most stable complex (**12a**) is the fastest one to give the carbamoyl adduct.

The different biological properties of **12a** and **15b** considered thus far clearly indicate that a long intermediate alkyl chain is favorable, while a long carbamic *N*-alkyl chain is less optimal for AChE inhibition. Looking at the K_C and k_3 values of **12a** and **15b** (Table 3), it might be hypothesized that these two structural features influence the carbamylation reaction more than the stability of the enzyme–inhibitor noncovalent complex. In any way, the *N*-alkyl carbamic side chain could increase the bulk of the molecule to an extent where the interaction with the active site is disturbed, despite the relatively wide dimensions of the gorge. The nucleophilic attack of the catalytic serine might be hampered, because of the steric hindrance around the carbamoyl group.

The unfavorable effects of the carbamic *N*-alkyl chain on AChE inhibition are reversed when considering BuChE inhibition. This is evident by comparing the IC_{50} values against the two enzymes in the series **15a–d**. A clue to interpret such a behavior might be provided by the consideration of the k_{obs} values determined for the inhibition of both enzymes by **15b**: 1.009 min^{-1} for BuChE carbamylation and 0.0243 min^{-1} for AChE carbamylation. BuChE is characterized by a wider gorge than AChE,¹⁹ and this might be the reason **15b** reacts faster with BuChE leading to a higher potency.

The results of the experiments of AChE activity regeneration (illustrated in Figure 4) carried out with **12a** and **15b**, two xanthone derivatives displaying different structural characteristics, suggest some observation about the terminal phase of the AChE-inhibitors interaction. The recovery of enzyme activity after inhibition by **12a** shows a biphasic time course,^{13b}

characterized by $t_{1/2}$ of 0.9 and 11.2 h, respectively. This behavior can be compared to that of physostigmine that bears the same methylcarbamic fragment as **12a**, even if on a different molecular skeleton. As previously reported,^{5b} in our system, the physostigmine-inhibited AChE recovers its activity with $t_{1/2} = 1.6$ h, which implies some difference in the regeneration mechanisms, despite the identity of the hydrolyzed carbamoyl fragments. The hypothesis might be advanced that the released alcoholic moieties of the two inhibitors (eseroline from physostigmine, 3-[*N*-methyl-*N*-(3-hydroxybenzyl)amino]hexyloxyxanthen-9-one (**3a**) from **12a**) have some different residual binding affinity for a secondary site in the AChE gorge, that contributes to a longer lasting inhibition.

With regards to the dramatically longer duration of action of the 7-morpholinoheptyl-derivative **15b** (no enzyme regeneration after 96 h), it is not a surprise at the light of a similar result obtained with an *N*-heptyl carbamate belonging to the series previously studied.^{5b} Also, the recently solved crystal structure of a carbamoylated AChE⁹ showed that the substantial irreversibility of the inhibitory action of 8-(2,6-dimethylmorpholino)octylcarbamoyleseroline (MF268) might be ascribed to limited access of hydrolytic water molecules to the carbamoylated active site, in consequence of the filling of the AChE gorge by the long carbamic residue. Such steric hindrance is further reinforced by the π -cation interaction of the dimethylmorpholino group with the Trp279 residue that anchors the hydrolyzed fragment within the enzyme cavity. It is reasonable to assume that the 7-morpholinoheptylcarbamoyl residue of **15b** exerts similar effects, thus leading to the extremely slow reactivation of the inhibited enzyme.

Conclusions

In this paper, the SAR of ω -[*N*-methyl-*N*-(3-alkylcarbamoyloxyphenyl)methyl]aminoalkoxyaryl AChE and BuChE inhibitors were studied by the synthesis and biological characterization of a series of purposely designed analogues. The effects of different molecular fragments on the AChE and BuChE inhibitory potency were determined and were also discussed on the basis of some structural and physicochemical properties. The SAR considerations were integrated with the results of a previous article^{5b} dealing with the same class of carbamic cholinesterase inhibitors.

The steps of the pseudoirreversible mechanism of AChE inhibition by two representative compounds were studied through the determination of the kinetic and thermodynamic constants. The kinetic data allowed for enlightenment of the role played by the variation of the alkyl chain in two different positions of the molecular skeleton in directing selectivity, affinity, and duration of action of this kind of AChE inhibitors. The prolonged duration of the anticholinesterase effect of the morpholino and long alkyl chain derivatives should provide the basis for their higher therapeutic potential.

Experimental Section

Chemistry. General Methods. All melting points were determined in open glass capillaries, using a Büchi apparatus, and are uncorrected. ¹H NMR spectra were recorded in CDCl₃ solution on a Varian Gemini 300 spectrometer, with Me₄Si as internal standard. Wherever analyses are only indicated with

element symbols, analytical results obtained for those elements are within 0.4% of the theoretical values.

3-(6-Chlorohexyloxy)xanthen-9-one (1a). A stirred suspension of 2.12 g (0.01 mol) of 3-hydroxyxanthen-9-one, 3.9 g (0.02 mol) of 1-bromo-6-chlorohexane, and 1.4 g (0.01 mol) of K₂CO₃ in dry acetone was refluxed for 24 h. The reaction was monitored by TLC. The hot reaction mixture was filtered and evaporated to dryness. The residue was crystallized from toluene to give 2.3 g (70%) of **1a**: mp 96–97 °C. ¹H NMR δ 1.5 (m, 4H), 1.85 (m, 4H), 3.55 (t, 2H), 4.05 (t, 2H), 6.85–8.35 (m, 7H, Ar). Anal. (C₁₉H₁₉ClO₃): C, H.

3-(7-Bromoheptyloxy)xanthen-9-one (1b). Using the previous procedure and starting from 2.12 g (0.01 mol) of 3-hydroxyxanthen-9-one and 5.18 g (0.02 mol) of 1,7-dibromoheptane, 2.1 g (70%) of **1b** was obtained: mp 90–93 °C (toluene). ¹H NMR δ 1.5 (m, 6H), 1.85 (m, 4H), 3.45 (t, 2H), 4.1 (t, 2H), 6.85–8.35 (m, 7H, Ar). Anal. (C₂₀H₂₁BrO₃): C, H.

3-(8-Bromooctyloxy)xanthen-9-one (1c). Using the previous procedure and starting from 2.12 g (0.01 mol) of 3-hydroxyxanthen-9-one and 5.44 g (0.02 mol) of 1,8-dibromooctane, 2.8 g (70%) of **1c** was obtained: mp 138–141 °C (toluene). ¹H NMR δ 1.5 (m, 8H), 1.85 (m, 4H), 3.45 (t, 2H), 4.1 (t, 2H), 6.85–8.35 (m, 7H, Ar). Anal. (C₂₁H₂₃BrO₃): C, H.

3-(9-Bromononyloxy)xanthen-9-one (1d). Using the previous procedure and starting from 2.12 g (0.01 mol) of 3-hydroxyxanthen-9-one and 5.72 g (0.02 mol) of 1,9-dibromononane, 3.3 g (80%) of **1d** was obtained: mp 100–102 °C (toluene). ¹H NMR δ 1.4 (m, 10H), 1.85 (m, 4H), 3.45 (t, 2H), 4.1 (t, 2H), 6.85–8.35 (m, 7H, Ar). Anal. (C₂₂H₂₅BrO₃): C, H.

3-(10-Bromodecyloxy)xanthen-9-one (1e). Using the previous procedure and starting from 2.12 g (0.01 mol) of 3-hydroxyxanthen-9-one and 6.0 g (0.02 mol) of 1,10-dibromodecane, 3.02 g (70%) of **1e** was obtained: mp 124–126 °C (toluene). ¹H NMR δ 1.4 (m, 12H), 1.85 (m, 4H), 3.45 (t, 2H), 4.1 (t, 2H), 6.85–8.35 (m, 7H, Ar). Anal. (C₂₃H₂₇BrO₃): C, H.

[4-(3-Chloropropoxy)phenyl](phenyl)methanone (1f). Using the previous procedure and starting from 1.98 g (0.01 mol) of 4-hydroxyphenyl(phenyl)methanone and 3.14 g (0.02 mol) of 1-bromo-3-chloropropane, 1.85 g (70%) of **1f** was obtained: mp 53–56 °C (ligroin). ¹H NMR δ 2.25 (m, 2H), 3.75 (t, 2H), 4.2 (t, 2H), 6.9–7.85 (m, 9H, Ar). Anal. (C₁₆H₁₅ClO₂): C, H.

1-Benzyl-3-(3-chloropropoxy)benzene (1g). Using the previous procedure and starting from 1.74 g (0.01 mol) of 3-benzylphenol, 1.82 g (70%) of **1g** was obtained: mp 37–39 °C (ligroin). ¹H NMR δ 2.3 (m, 2H), 3.8 (t, 2H), 4.0 (s, 2H), 4.15 (t, 2H), 6.9–7.4 (m, 9H, Ar). Anal. (C₁₆H₁₇ClO): C, H.

2-(3-Chloropropoxy)naphthalene (1h). Using the previous procedure and starting from 1.44 g (0.01 mol) of 2-naphthol, 1.5 g (70%) of **1h** was obtained: mp 48–50 °C (toluene). ¹H NMR δ 2.35 (m, 2H), 3.8 (t, 2H), 4.25 (t, 2H), 7.15–7.85 (m, 7H, Ar). Anal. (C₁₃H₁₃ClO): C, H.

1-(3-Chloropropoxy)benzene (1i). Using the previous procedure and starting from 0.94 g (0.01 mol) of phenol, 1.2 g (90%) of **1i** was obtained: oil. ¹H NMR δ 2.25 (m, 2H), 3.75 (t, 2H), 4.2 (t, 2H), 6.9–7.4 (m, 5H, Ar). Anal. (C₉H₁₁ClO): C, H.

4-(3-Chloropropoxy)biphenyl (1j). Using the previous procedure and starting from 1.46 g (0.01 mol) of 4-hydroxybiphenyl, 1.7 g (70%) of **1j** was obtained: mp 59–61 °C (ligroin). ¹H NMR δ 2.3 (m, 2H), 3.8 (t, 2H), 4.17 (t, 2H), 7.0–7.6 (m, 9H, Ar). Anal. (C₁₅H₁₅ClO): C, H.

3-(6-Iodohexyloxy)xanthen-9-one (2a). A mixture of 3.3 g (0.01 mol) of **1a** and 1.5 g (0.01 mol) of NaI in 30 mL of methyl ethyl ketone was refluxed for 4 h. After cooling, the separated solid was collected by filtration: 3.8 g (90%) of **2a** was obtained: mp 75–78 °C (ligroin). ¹H NMR δ 1.5 (m, 4H), 1.85 (m, 4H), 3.2 (t, 2H), 4.05 (t, 2H), 6.8–8.35 (m, 7H, Ar). Anal. (C₁₉H₁₉IO₃): C, H.

[4-(3-Iodopropoxy)phenyl](phenyl)methanone (2f). Using the previous procedure and starting from 2.74 g (0.01 mol) of **1f**, 2.9 g (80%) of **2f** was obtained: mp 199–203 °C. ¹H NMR δ 2.2 (m, 2H), 3.25 (t, 2H), 4.0 (t, 2H), 6.8–7.7 (m, 9H, Ar). Anal. (C₁₆H₁₅IO₂): C, H.

1-Benzyl-3-(3-iodopropoxy)benzene (2g). Using the previous procedure and starting from 2.6 g (0.01 mol) of **1g**, 2.8 g (80%) of **2g** was obtained: mp 56–59 °C (toluene). ¹H NMR δ 2.25 (m, 2H), 3.3 (t, 2H), 3.95 (s, 2H), 4.05 (t, 2H), 6.8–7.4 (m, 9H, Ar). Anal. (C₁₆H₁₇IO): C, H.

2-(3-Iodopropoxy)naphthalene (2h). Using the previous procedure and starting from 2.2 g (0.01 mol) of **1h**, 2.5 g (80%) of **2h** was obtained: mp 128–130 °C. ¹H NMR δ 2.25 (m, 2H), 3.35 (t, 2H), 4.1 (t, 2H), 7.0–7.7 (m, 7H, Ar). Anal. (C₁₃H₁₃IO): C, H.

1-(3-Iodopropoxy)benzene (2i). Using the previous procedure and starting from 1.7 g (0.01 mol) of **1i**, 2.3 g (90%) of **2i** was obtained: oil. ¹H NMR δ 2.25 (m, 2H), 3.35 (t, 2H), 4.0 (t, 2H), 6.9–7.4 (m, 5H, Ar). Anal. (C₉H₁₁IO): C, H.

4-(3-Iodopropoxy)biphenyl (2j). Using the previous procedure and starting from 2.46 g (0.01 mol) of **1j**, 2.4 g (70%) of **2j** was obtained: mp 60–61 °C (ligroin). ¹H NMR δ 2.3 (m, 2H), 3.4 (t, 2H), 4.1 (t, 2H), 7.0–7.6 (m, 9H, Ar). Anal. (C₁₅H₁₅IO): C, H.

3-[[[N-Methyl-N-(3-hydroxybenzyl)amino]hexyl]oxy]xanthen-9-one (3a). A solution of 2.1 g (0.005 mol) of **2a** and 1.37 g (0.01 mol) of N-(3-hydroxybenzyl)methylamine in 100 mL of toluene was refluxed for 15 h. After cooling, the reaction mixture was washed (H₂O), dried (Na₂SO₄), and evaporated to dryness. The residue, on crystallizing from toluene, afforded 0.86 g (40%) of **3a**: mp 92–95 °C. ¹H NMR δ 1.4 (m, 6H), 1.8 (m, 2H), 2.2 (s, 3H), 2.4 (t, 2H), 3.45 (s, 2H), 4.05 (t, 2H), 6.7–8.35 (m, 11H, Ar). Anal. (C₂₇H₂₉NO₄): C, H, N.

3-[[[N-Methyl-N-(3-hydroxybenzyl)amino]heptyl]oxy]xanthen-9-one (3b). Using the previous procedure and starting from 1.94 g (0.005 mol) of **1b**, 0.89 g (40%) of **3b** was obtained: mp 107–110 °C. ¹H NMR δ 1.4 (m, 8H), 1.8 (m, 2H), 2.2 (s, 3H), 2.4 (t, 2H), 3.45 (s, 2H), 4.05 (t, 2H), 6.7–8.35 (m, 11H, Ar). Anal. (C₂₈H₃₁NO₄): C, H, N.

3-[[[N-Methyl-N-(3-hydroxybenzyl)amino]octyl]oxy]xanthen-9-one (3c). Using the previous procedure and starting from 2.01 g (0.005 mol) of **1c**, 0.92 g (40%) of **3c** was obtained: mp 110–112 °C. ¹H NMR δ 1.4 (m, 10H), 1.8 (m, 2H), 2.2 (s, 3H), 2.4 (t, 2H), 3.45 (s, 2H), 4.05 (t, 2H), 6.7–8.4 (m, 11H, Ar). Anal. (C₂₉H₃₃NO₄): C, H, N.

3-[[[N-Methyl-N-(3-hydroxybenzyl)amino]nonyl]oxy]xanthen-9-one (3d). Using the previous procedure and starting from 2.08 g (0.005 mol) of **1d**, 0.94 g (40%) of **3d** was obtained: mp 82–85 °C. ¹H NMR δ 1.4 (m, 12H), 1.8 (m, 2H), 2.2 (s, 3H), 2.4 (t, 2H), 3.45 (s, 2H), 4.05 (t, 2H), 6.7–8.35 (m, 11H, Ar). Anal. (C₃₀H₃₅NO₄): C, H, N.

3-[[[N-Methyl-N-(3-hydroxybenzyl)amino]decyl]oxy]xanthen-9-one (3e). Using the previous procedure and starting from 2.15 g (0.005 mol) of **1e**, 0.97 g (40%) of **3e** was obtained, mp 89–91 °C. ¹H NMR δ 1.4 (m, 14H), 1.8 (m, 2H), 2.2 (s, 3H), 2.4 (t, 2H), 3.45 (s, 2H), 4.05 (t, 2H), 6.7–8.35 (m, 11H, Ar). Anal. (C₃₁H₃₇NO₄): C, H, N.

4-[[N-Methyl-N-(3-hydroxybenzyl)amino]propoxy]phenyl(phenyl)methanone (3f). Using the previous procedure and starting from 1.37 g (0.005 mol) of **2f**, 0.75 g (40%) of **3f** was obtained as hydrochloride salt: mp 151–153 °C (MeOH/ether). ¹H NMR δ 2.0 (m, 2H), 2.2 (s, 3H), 2.55 (t, 2H), 3.45 (s, 2H), 4.05 (t, 2H), 6.7–7.9 (m, 13H, Ar). Anal. (C₂₄H₂₆ClNO₃): C, H, N.

3-[[[3-(3-Benzylphenoxy)propyl](methyl)amino]methyl]phenol (3g). Using the previous procedure and starting from 1.3 g (0.005 mol) of **2g**, 0.72 g (40%) of **3g** was obtained: mp 72–75 °C. ¹H NMR δ 2.0 (m, 2H), 2.2 (s, 3H), 2.6 (t, 2H), 3.45 (s, 2H), 3.95 (m, 4H), 6.7–7.3 (m, 13H, Ar). Anal. (C₂₄H₂₇NO₂): C, H, N.

3-[[[Methyl][3-(2-naphthoxy)propyl]amino]methyl]phenol (3h). Using the previous procedure and starting from 1.1 g (0.005 mol) of **2h**, 0.64 g (40%) of **3h** was obtained: mp 80–84 °C. ¹H NMR δ 2.15 (m, 2H), 2.35 (s, 3H), 2.8 (t, 2H), 3.7 (s, 2H), 4.05 (t, 2H), 6.7–7.8 (m, 11H, Ar). Anal. (C₂₁H₂₃NO₂): C, H, N.

3-[[[Methyl(3-phenoxypropyl)amino]methyl]phenol (3i). Using the previous procedure and starting from 0.85 g (0.005 mol) of **2i**, 0.81 g (60%) of **3i** was obtained: mp 78–80

°C. ¹H NMR δ 2.15 (m, 2H), 2.35 (s, 3H), 2.7 (t, 2H), 3.6 (s, 2H), 4.0 (t, 2H), 6.0 (broad, 1H, OH), 6.7–7.7 (m, 9H, Ar). Anal. (C₁₇H₂₁NO₂): C, H, N.

4-[3-[N-Methyl-N-(3-hydroxybenzyl)amino]propoxy]biphenyl (3j). Using the previous procedure and starting from 1.23 g (0.005 mol) of **2j**, 0.81 g (45%) of **3j** was obtained: mp 78 °C. ¹H NMR δ 2.1 (m, 2H), 2.27 (s, 3H), 2.6 (t, 2H), 2.7 (broad, 1H, OH), 3.5 (s, 2H), 4.1 (t, 2H), 6.7–7.6 (m, 9H, Ar). Anal. (C₂₄H₂₇NO₂): C, H, N.

3-(Propargyloxy)xanthen-9-one (4). A stirred suspension of 2.12 g (0.01 mol) of 3-hydroxyxanthen-9-one, 1.2 g (0.01 mol) of propargyl bromide, 1.4 g (0.01 mol) of K₂CO₃ in dry acetone was refluxed for 24 h. The reaction was monitored by TLC. The hot reaction mixture was filtered and evaporated to dryness. The residue was crystallized from toluene to give 2.25 g (90%) of **4**, mp 142–144 °C. ¹H NMR δ 2.6 (m, 1H), 4.84 (m, 2H), 6.98–8.35 (m, 7H, Ar). Anal. (C₁₆H₁₀O₃): C, H.

3-[[4-[N-Methyl-N-(3-benzyloxybenzyl)amino]-2-butynyl]oxy]xanthen-9-one (5). A solution of 1.15 g (4.6 mmol) of **4** in EtOH/H₂O 1:1 (15 mL) was added to a suspension of CuSO₄ (0.1 g), HCHO (0.5 mL), and 1.36 g (6.0 mmol) of N-(3-benzyloxybenzyl)methylamine. H₂SO₄ was added until pH 8, and the mixture was refluxed for 24 h. After cooling, 30 mL NH₃ was added, and the reaction mixture was extracted with ether, dried (Na₂SO₄), and evaporated to dryness. The residue purified by flash chromatography afforded 1.7 g (60%) of **5**, oil. ¹H NMR δ 2.3 (s, 3H), 3.4 (s, 2H), 3.55 (s, 2H), 4.9 (s, 2H), 5.15 (s, 2H), 6.8–8.4 (m, 16H, Ar). Anal. (C₃₂H₂₇NO₄): C, H, N.

3-[[4-[N-Methyl-N-(3-hydroxybenzyl)amino]-2-butynyl]oxy]xanthen-9-one (6). A solution of 1.7 g (3.48 mmol) of **5** in dry CH₂Cl₂ (35 mL) was stirred under N₂ at 0 °C; N,N-dimethylaniline (8.3 mL) was added, and the mixture was stirred for 5 min. Then 1.8 g (14 mmol) of anhydrous AlCl₃ was added, and the reaction was stirred at room temperature for 6 h. The reaction mixture was quenched with H₂O, and the organic layer was washed with H₂O, dried (Na₂SO₄), and evaporated to dryness. The residue was purified by flash chromatography, affording 0.8 g (60%) of **6**: mp 195–197 °C. ¹H NMR δ 2.25 (s, 3H), 3.3 (s, 2H), 3.45 (s, 2H), 4.85 (s, 2H), 6.7–8.4 (m, 11H, Ar). Anal. (C₂₅H₂₁NO₄): C, H, N.

3-[3-(7-Nitro-1,2,3,4-tetrahydro-2-isoquinolyl)propoxy]xanthen-9-one (9). To a solution of 3.8 g (0.01 mol) of **7**^{5b} in toluene was added 3.56 g (0.02 mol) of 7-nitro-1,2,3,4-tetrahydroisoquinoline,¹¹ and the solution was refluxed for 12 h. The reaction mixture was washed with H₂O, dried (Na₂SO₄), and evaporated to dryness. The residue purified by flash chromatography (dichloromethane/ethyl acetate 3:2) afforded 1.3 g (30%) of **9**: mp 144–145 °C (toluene). ¹H NMR δ 2.08–2.23 (m, 2H), 2.71–2.87 (m, 4H), 3.04 (t, 2H), 3.78 (s, 2H), 4.22 (t, 2H), 6.9–8.3 (m, 10H, Ar). Anal. (C₂₅H₂₂N₂O₅): C, H, N.

3-[3-(7-Amino-1,2,3,4-tetrahydro-2-isoquinolyl)propoxy]xanthen-9-one (10). A solution of 2.15 g (0.005 mol) of **9** in tetrahydrofuran (150 mL) was hydrogenated at room temperature and atmospheric pressure over palladium on carbon. The catalyst was filtered off, and the mixture was evaporated to dryness. The residue was crystallized from toluene to yield 1.8 g (90%) of **10**: mp 126–127 °C. ¹H NMR δ 2.05–2.21 (m, 2H), 2.63–2.85 (m, 6H), 3.58 (s, 2H), 4.19 (t, 2H), 6.4–8.3 (m, 10H, Ar). Anal. (C₂₅H₂₄N₂O₃): C, H, N.

3-[3-(7-Hydroxy-1,2,3,4-tetrahydro-2-isoquinolyl)propoxy]xanthen-9-one (11). A solution of 2.0 g (0.005 mol) of **10** in 20 mL of H₂SO₄ and 40 mL of H₂O was cooled to –5 °C, and a solution of 0.34 g (0.005 mol) of NaNO₂ in 5 mL of H₂O was added dropwise. The solution was stirred for 30 min, then poured in H₂SO₄ 1:2 (150 mL), and stirred in a steam bath for 30 min. The mixture was allowed to stand overnight, and the resulting precipitate was collected by filtration, washed with H₂O, and crystallized from ethanol to give 0.8 g (40%) of **11**: mp 193–194 °C. ¹H NMR δ 2.06–2.18 (m, 2H), 2.61–2.88 (m, 6H), 3.62 (s, 2H), 4.20 (t, 2H), 6.8–8.3 (m, 10H, Ar). Anal. (C₂₅H₂₃NO₄): C, H, N.

General Method for the Preparation of Carbamates (12a–12j, 13, 14, 15a–d). A mixture of the selected ω-[N-

alkyl-*N*-(3-hydroxy)benzylaminoalkoxy derivative (0.001 mol), the selected alkyl isocyanate (0.001 mol), and 10 mg of NaH in dry toluene was stirred at room temperature for 24 h, quenched with water, and then extracted with dichloromethane. The organic layer was washed with water, dried, and evaporated to dryness. The residue was purified by crystallization or by flash chromatography.

¹H NMR for Compounds 12a–12j, 13, 14, 15a–d.

12a: δ (CDCl₃) 1.45 (m, 6H), 1.75 (m, 2H), 2.1 (s, 3H), 2.3 (t, 2H), 2.8 (d, 3H), 3.4 (s, 2H), 4.0 (t, 2H), 4.85 (broad, 1H, NH), 6.8–8.3 (m, 11H, Ar). **12b:** δ (CDCl₃) 1.5 (m, 8H), 1.85 (m, 2H), 2.2 (s, 3H), 2.35 (t, 2H), 2.8 d, 3H), 3.5 (s, 2H), 4.1 (t, 2H), 4.9 (broad, 1H, NH), 6.8–8.35 (m, 11H, Ar). **12c:** δ (CDCl₃) 1.45 (m, 10H), 1.75 (m, 2H), 2.1 (s, 3H), 2.3 (t, 2H), 2.8 (d, 3H), 3.4 (s, 2H), 4.0 (t, 2H), 4.85 (broad, 1H, NH), 6.8–8.3 (m, 11H, Ar). **12d:** δ (CDCl₃) 1.45 (m, 12H), 1.75 (m, 2H), 2.1 (s, 3H), 2.3 (t, 2H), 2.8 (d, 3H), 3.4 (s, 2H), 4.0 (t, 2H), 4.85 (broad, 1H, NH), 6.8–8.3 (m, 11H, Ar). **12e:** δ (CDCl₃) 1.45 (m, 14H), 1.8 (m, 2H), 2.15 (s, 3H), 2.35 (t, 2H), 2.8 (d, 3H), 3.4 (s, 2H), 4.1 (t, 2H), 4.95 (broad, 1H, NH), 6.8–8.4 (m, 11H, Ar). **12f:** δ (DMSO-*d*₆) 2.25 (t, 2H), 2.65 (d, 3H), 2.7 (s, 3H), 3.2 (t, 2H), 4.1–4.5 (m, 4H), 7.0–7.8 (m, 13H, Ar). **12g:** δ (DMSO-*d*₆) 2.15 (t, 2H), 2.65 (d, 3H), 2.7 (s, 3H), 3.2 (t, 2H), 3.85 (s, 2H), 4.0 (t, 2H), 4.3 (m, 2H), 6.8–7.8 (m, 13H, Ar). **12h:** δ (DMSO-*d*₆) 2.25 (t, 2H), 2.65 (d, 3H), 2.75 (s, 3H), 3.2 (t, 2H), 4.1–4.5 (m, 4H), 7.1–7.9 (m, 11H, Ar). **12i:** δ (DMSO-*d*₆) 2.25 (t, 2H), 2.65 (d, 3H), 2.7 (s, 3H), 3.2 (t, 2H), 4.3 (m, 2H), 6.9–7.8 (m, 9H, Ar). **12j:** δ (CDCl₃) 2.0 (m, 2H), 2.25 (s, 3H), 2.6 (t, 2H), 2.87 (d, 3H), 3.55 (s, 2H), 4.08 (t, 2H), 6.95–7.58 (m, 13H, Ar). **13:** δ (DMSO-*d*₆) 2.65 (s, 3H), 2.75 (d, 3H), 4.1 (s, 2H), 4.3 (s, 2H), 5.2 (s, 2H), 7.1–8.2 (m, 11H, Ar). **14:** δ (CDCl₃) 2.24–2.43 (m, 2H), 2.66 (d, 3H), 3.29–3.48 (m, 4H), 3.71–3.83 (m, 2H), 4.25–4.68 (m, 4H), 7.04–8.12 (m, 10H, Ar), 10.80 (broad, 1H, NH). **15a:** δ (CDCl₃) 1.2–1.6 (m, 8H), 2.05 (t, 2H), 2.3 (m, 5H), 2.45 (m, 4H), 2.6 (t, 2H), 3.25 (m, 2H), 3.55 (s, 2H), 3.75 (m, 4H), 4.2 (t, 2H), 5.05 (broad, 1H, NH), 6.8–8.4 (m, 11H, Ar). **15b:** δ (CDCl₃) 1.3–1.6 (m, 10H), 2.05 (t, 2H), 2.3 (m, 5H), 2.45 (m, 4H), 2.6 (t, 2H), 3.25 (m, 2H), 3.55 (s, 2H), 3.75 (m, 4H), 4.2 (t, 2H), 5.0 (broad, 1H, NH), 6.9–8.4 (m, 11H, Ar). **15c:** δ (CDCl₃) 1.2–1.6 (m, 12H), 2.05 (t, 2H), 2.3 (m, 5H), 2.45 (m, 4H), 2.55 (t, 2H), 3.25 (m, 2H), 3.5 (s, 2H), 3.7 (m, 4H), 4.2 (t, 2H), 5.0 (broad, 1H, NH), 6.8–8.4 (m, 11H, Ar). **15d:** δ (CDCl₃) 1.2–1.6 (m, 14H), 2.05 (t, 2H), 2.3 (m, 5H), 2.45 (m, 4H), 2.55 (t, 2H), 3.25 (m, 2H), 3.5 (s, 2H), 3.7 (m, 4H), 4.2 (t, 2H), 5.0 (broad, 1H, NH), 6.8–8.4 (m, 11H, Ar).

Inhibition of AChE and BuChE. The method of Ellman¹² was followed. ATCh iodide solution (0.037 M) was prepared in water. 5,5'-Dithiobis(2-nitrobenzoic acid) (DTNB, Ellman's reagent) (0.01 M) was dissolved in pH 7.0 phosphate buffer, and 0.15% (w/v) NaHCO₃ was added. AChE solution was prepared dissolving 20 units in 5 mL of 0.2% aqueous gelatin by sonication at 35 °C. A dilution 1:1 with water was performed before use, to obtain the enzyme activity comprised between 0.13 and 0.100 AU/min. Stock solutions of the test compounds (0.5–1 mM) were prepared in ethanol as well as the physostigmine reference stock solution. The assay solutions were prepared by diluting the stock solutions in water. Five different concentrations of each compound were used in order to obtain inhibition of AChE activity comprised between 20 and 80%.

The assay solution consisted of a 0.1 M phosphate buffer pH 8.0, with the addition of 340 μ M DTNB, 0.035 unit/mL AChE derived from human erythrocytes (Sigma Chemical), and 550 μ M ATCh iodide. The final assay volume was 1 mL. Test compounds were added to the assay solution and preincubated with the enzyme for 20 min, the addition of substrate following.

Initial rate assays were performed at 37 °C with a Jasco Uvidec-610 double beam spectrophotometer: the rate of absorbance increase at 412 nm was followed for 5 min. Assays were performed with a blank containing all components except AChE, to account for nonenzymatic reaction. The reaction rates were compared, and the percent inhibition due to the presence of test compounds was calculated. Each concentration

was analyzed in triplicate. The percent inhibition of the enzyme activity due to the presence of increasing test compound concentration was calculated by the following expression: $100 - (v_i/v_0 \times 100)$, where v_i is the rate calculated in the presence of inhibitor and v_0 is the enzyme activity. Inhibition curves were obtained for each compound by plotting the percent inhibition versus the logarithm of inhibitor concentration in the assay solution. The linear regression parameters were determined for each curve and the IC₅₀ extrapolated.

Inhibition of BuChE was measured as described above, substituting 0.035 unit/mL of BuChE from human serum and 550 μ M butyrylthiocholine (BuTCh) for enzyme and substrate, respectively.

Kinetic characterization of carbamoylation events. The stopped time assay was performed, in which AChE and inhibitors at five concentrations comprised in the range 0.34–1.35 nM (**12a**), 0.81–57 nM (**15b**), and 10–200 nM (physostigmine as reference compound) were mixed in the assay buffer at pH 8.0. After few minutes incubation at 37 °C, the determination of residual activity of the AChE-catalyzed hydrolysis of ATCh was followed spectrophotometrically at 412 nm. A parallel control (i.e., no inhibitors in the mixture) allowed to adjust activities measured at various time.

The data were fitted to eq 1, and k_{obs} values were calculated accordingly. K_C and k_3 values were calculated from the plots of k_{obs} against [I] (eq 2).

Decarbamoylation Kinetics. Stock solutions in replicates were prepared as following: the free enzyme (1.0 units in 2 mL of 0.1 M phosphate buffer pH 8.0), the same amount of enzyme plus **12a** (1.39×10^{-8} M) and **15b** (2.6×10^{-7} M).

The solutions were gently stirred and incubated at 37 °C for 20 min. They were then loaded into 12,000 MW cutoff dialysis bags and dialyzed at 4 °C against 2 L of 0.1 M phosphate buffer pH 8.0. Dialysis was interrupted after 6–12–18–24–48–96 h. The solutions were diluted five times with the same buffer and kept at 20–22 °C under magnetic stirring. Aliquots of 0.95 mL of each solution were sampled, and the enzyme activity was spectrophotometrically tested after addition of 0.034 mL of DTNB and 0.016 mL of ATCh as above-described. Plots of enzyme activities for each compound expressed as a percentage of the dialyzed free enzyme activity against the time of dialysis were calculated for each inhibitors. The obtained curves were fitted to one phase exponential growth or two phase exponential growth with the Prism 3.0 program and the experimental rate constants k_5 derived. Half time is $0.69/k_5$.

Acknowledgment. Investigation supported by University of Bologna (funds for selected research topics) and by MURST. M.R. thanks Corwin Hansch for the access to the C-QSAR program.

References

- Selkoe, D. J. Translating Cell Biology into Therapeutic Advances in Alzheimer's Disease. *Nature* **1999**, *399*, A23–A31.
- Siddiqui, M. F.; Levey, A.-I. Cholinergic Therapies in Alzheimer's Disease. *Drugs Fut.* **1999**, *24*, 417–424.
- Bartus, R. T.; Dean, L. D. III; Beer, B.; Lippa, A. S. The Cholinergic Hypothesis of Geriatric Memory Dysfunction. *Science* **1982**, *217*, 408–417.
- Reiner, E.; Radić, Z. Mechanism of Action of Cholinesterase Inhibitors. In *Cholinesterases and Cholinesterase Inhibitors*; Giacobini, E., Ed.; Martin Dunitz Ltd: London, UK, 2000; pp 103–119.
- (a) Valenti, P.; Rampa, A.; Bisi, A.; Fabbri, G.; Andrisano, V.; Cavrini, V. Cholinergic Agents. Synthesis and Acetylcholinesterase Inhibitory Activity of Some ω -[*N*-Methyl-*N*-(3-alkyl-carbamoyloxyphenyl)methyl]aminoalkoxyxanthen-9-ones. *Med. Chem. Res.* **1995**, *5*, 255–264. (b) Rampa, A.; Bisi, A.; Valenti, P.; Recanatini, M.; Cavalli, A.; Andrisano, V.; Cavrini, V.; Fin, L.; Buriani, A.; Giusti, P. Acetylcholinesterase Inhibitors: Synthesis and Structure–Activity Relationships of ω -[*N*-methyl-*N*-(3-alkylcarbamoyloxyphenyl)methyl]aminoalkoxyheteroaryl derivatives. *J. Med. Chem.* **1998**, *41*, 3976–3986.

- (6) Harel, M.; Schalk, I.; Ehret-Sabatier, L.; Bouet, F.; Goeldner, M.; Hirth, C.; Axelsen, P. H.; Silman, I.; Sussman, J. L. Quaternary Ligand Binding to Aromatic Residues in the Active-Site Gorge of Acetylcholinesterase. *Proc. Natl. Acad. Sci. U.S.A.* **1993**, *90*, 9031–9035.
- (7) Inestrosa, N. C.; Alvarez, A.; Pérez, C. A.; Moreno, R. D.; Vicente, M.; Linker, C.; Casanueva, O. I.; Soto, C.; Garrido, J. Acetylcholinesterase Accelerates Assembly of Amyloid- β -Peptides into Alzheimer's Fibrils: Possible Role of the Peripheral Site of the Enzyme. *Neuron* **1996**, *16*, 881–891.
- (8) Perola, E.; Cellai, L.; Lamba, D.; Filocamo, L.; Brufani, M. Long Chain Analogues of Physostigmine as Potential Drugs for Alzheimer's Disease: New Insights into the Mechanism of Action in the Inhibition of Acetylcholinesterase. *Biochim. Biophys. Acta* **1997**, *1343*, 41–50.
- (9) Bartolucci, C.; Perola, E.; Cellai, L.; Brufani, M.; Lamba, D. "Back Door" Opening Implied by the Crystal Structure of a Carbamoylated Acetylcholinesterase. *Biochemistry* **1999**, *38*, 5714–5719.
- (10) Alisi, M. A.; Brufani, M.; Filocamo, L.; Gostoli, G.; Licandro E.; Cesta, M. C.; Lappa, S.; Marchesini, D.; Pagella P. Synthesis and Structure–Activity Relationships of New Acetylcholinesterase Inhibitors: Morpholinoalkylcarbamoyloxyeseroline Derivatives. *Bioorg. Med. Lett.* **1995**, *5*, 2077–2080.
- (11) McCoubrey, A.; Mathieson, D. W. *iso*Quinoline. Part III. The Nitration of 3:4-Dihydro- and 1:2:3:4-Tetrahydro-isoquinolines. *J. Chem. Soc.* **1951**, 2851–2853.
- (12) Ellman, G. L.; Courtney, K. D.; Andres, V.; Featherstone, R. M. A New and Rapid Colorimetric Determination of Acetylcholinesterase Activity. *Biochem. Pharmacol.* **1961**, *7*, 88–95.
- (13) (a) Main, A. R.; Hastings, F. L. Carbamylation and Binding Constants for the Inhibition of Acetylcholinesterase by Physostigmine. *Science* **1966**, *154*, 400–402. (b) Feaster, S. R.; Quinn, D. M. Mechanism-Based Inhibitors of Mammalian Cholesterol Esterase. *Methods Enzymol.* **1997**, *286*, 231–252. (c) Ariel, N.; Ordentlich, A.; Barak, D.; Bino, T.; Velan, B.; Shafferman, A. The Aromatic Patch of Three Proximal Residues in the Human Acetylcholinesterase Active Centre Allows for Versatile Interaction Modes with Inhibitors. *Biochem. J.* **1998**, *335*, 95–102.
- (14) Greig, N. H.; Pei, X.-F.; Soncrant, T. T.; Ingram, D. K.; Brossi, A. Phenserine and Ring C Hetero-Analogues: Drug Candidates for the Treatment of Alzheimer's Disease. *Med. Res. Rev.* **1995**, *15*, 3–31.
- (15) C-QSAR, Ver. 4.12; BioByte Corp.: Claremont, CA, 2000.
- (16) Yu, Q. S.; Atack, J. R.; Rapoport, S. I.; Brossi, A. Carbamate Analogues of (–)-Physostigmine: In Vitro Inhibition of Acetyl- and Butyryl-cholinesterase. *FEBS Lett.* **1988**, *234*, 127–130.
- (17) Yu, Q. S.; Holloway, H. W.; Utsuki, T.; Brossi, A.; Greig, N. H. Synthesis of Novel Phenserine-Based-Selective Inhibitors of Butyrylcholinesterase for Alzheimer's Disease. *J. Med. Chem.* **1999**, *42*, 1855–1861.
- (18) Giacobini, E. Cholinesterase Inhibitors: from the Calabar Bean to Alzheimer Therapy. In *Cholinesterases and Cholinesterase Inhibitors*; Giacobini, E., Ed.; Martin Dunitz Ltd: London, UK, 2000; pp 181–226.
- (19) Massoulié, J.; Sussman, J.; Bon, S.; Silman, I. Structure and Functions of Acetylcholinesterase and Butyrylcholinesterase. *Prog. Brain Res.* **1993**, *98*, 139–146.
- (20) Stewart, J. J. P. Optimization of Parameters for Semiempirical Methods. I. Methods. *J. Comput. Chem.* **1989**, *10*, 209–220.

JM010914B